

# Efficient Sampling of Transition Constraints for Motion Planning under Sliding Contacts

Marie-Therese Khouri<sup>1</sup>Andreas Ortrey<sup>2</sup>Marc Toussaint<sup>2,3</sup>

**Abstract**— Contact-based motion planning for manipulation, object exploration or balancing often requires finding sequences of fixed and sliding contacts and planning the transition from one contact in the environment to another. However, most existing algorithms do not take sliding contacts into account or consider them only for specialized scenarios. We propose a method to extend constraint-based planning framework using contact transitions for sliding contacts. Such transitions are elementary operations required for whole contact sequences. To model sliding contacts, we define a sliding contact constraint that permits the robot to slide on the surface of an object. To exploit transitions between sliding contacts, we develop a contact transition sampler, which uses three constraint modes: contact with a start surface, no contact and contact with a goal surface. We sample these transition modes uniformly which makes them usable with sampling-based planning algorithms. Our method is evaluated by testing it on manipulator arms of two, three and seven internal degrees of freedom with different objects and various sampling-based planning algorithms. This demonstrates that sliding contact constraints could be used as an elementary method for planning long-horizon contact sequences for high-dimensional robotic systems.

## I. INTRODUCTION

Robots that act in the real-world often require the use of contacts. Contacts are important to locomote by walking [11], [30], [3] or climbing [4], to manipulate the environment [37] or to grasp objects [6]. Algorithms that enable robots to move using contacts are studied in the field of contact-based motion planning [11], [36], [20]. The objective of contact-based motion planning is to complete a manipulation or locomotion task by reaching a goal configuration while incorporating contact constraints where chosen points on the robot have to be in contact with chosen surfaces in the environment.

One approach to deal with contact constraints is projection-based constraint planning [2], [20]. In projection-based constraint planning, we implicitly define contact constraints, which we can sample using dedicated projection methods [2]. Such a framework has been used to plan contact motions for the Robonaut 2 robot [20]. While projection-based planning works well for fixed contact planning [20], there does not yet exist an extension to incorporate sliding constraints or transitions between sliding contacts. Sliding contacts however, are a fundamental requirement if we want to explore the shape of an object [10], adjust an object grasp

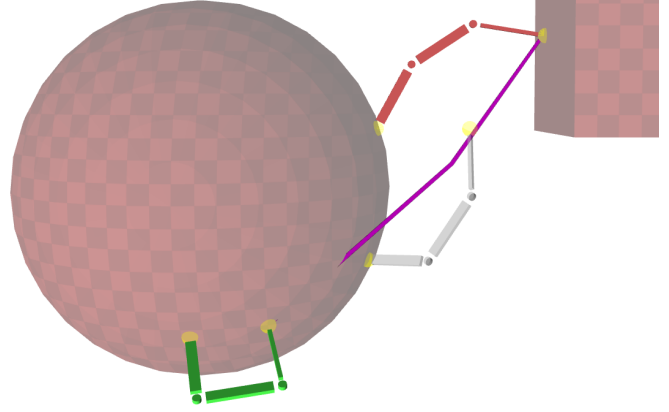


Fig. 1. We present a framework to plan sliding contact constraints on arbitrary mesh surfaces, where predefined contact points of a robot (yellow) are required to stay in constant contact with a surface.

[34], keep the robot in balance [33], minimize state uncertainty [31], plan more efficiently [32] or animate computer characters [16].

To overcome those limitations of constraint planning, we develop an extension of constraint planning for sliding contacts. This extension consists of the following items:

- 1) Definition of sliding-contact constraint and sliding-contact transition constraint by extending the constraint-based planning framework [20].
- 2) Sampling method for the transition constraint, which use constraint modes for efficient sampling.
- 3) Evaluations with various sampling-based planning algorithms for one-step cycles using manipulator arms with two, three or seven internal degrees-of-freedom (dof).

We concentrate in this paper exclusively on one-step sliding contact cycles, because solving such cycles robustly is of fundamental importance for planning long-horizon contact sequences [37].

## II. RELATED WORK

Planning contact sequences through an environment can be addressed using constraint-based motion planning [2], [20]. This approach is based on building probabilistic road maps or trees by randomly sampling configurations, which are projected onto the contact constraints to make them feasible [2]. The transition between contact constraints is often captured using a constraint graph [27], through which we can identify sequences of contacts to reach a goal [11].

<sup>1</sup>University of Stuttgart, Stuttgart, Germany  
marietheresekhoury@googlemail.com

<sup>2</sup>Max Planck Institute for Intelligent Systems, Stuttgart, Germany

<sup>3</sup>Technical University of Berlin, Berlin, Germany

Such sequences are often used to plan more complicated contact or manipulation tasks [13], [37]. Because contact constraints can often not be described analytically, we have to either learn them [12] or use methods to project onto them [2]. To plan longer contact sequences, it often becomes necessary to exploit the structure of the state space. Different approaches exist, for example by factoring the state space for more efficient sampling [39], by computing guide paths from a simplified robot geometry [36] or by precomputing convex regions in workspace which we can exploit using mixed-integer programming [8]. Our approach is complementary, in that we add sliding transition constraints to the constraint-based framework [20], which makes it possible to plan sliding transition constraints using sampling-based planner [23] or asymptotically optimal planner [17].

While constraint-based planning is often used to plan non-sliding contacts, there exists substantial research on the control aspect of sliding motions [38], [7]. To execute and control sliding motions, we could use physical models which make use of friction cone models [33] to directly optimize sliding motions to push objects along planar surfaces [37]. An alternative approach would be to learn the parameters of a controller for specific object categories [25]. Recent results using learned sliding controllers can be used for dexterous in-hand manipulation, where objects are either rotated in-hand without making contact with the environment [22], [1] or features in the environment are used as helper tools [7]. Our approach is complementary, in that we make simplifying assumptions on the control of sliding contacts (deterministic, no uncertainty) and concentrate on the computational challenges of planning sliding contacts [24], which could be used to provide guarantees on completeness and optimality.

### III. BACKGROUND

This section provides some background knowledge. Large parts of this section are based on Part II of [23] and [19].

A **configuration**  $q$  defines the independent variables of a given robot needed to uniquely specify the robot's position relative to a reference frame. Considering a manipulator arm with  $m$  number of rigid links connected by  $n$  joints that is fixed at one end, one possible configuration would define  $n$  internal variables plus external variables to describe a root frame fixed to the robot. The **configuration space**  $Q$  of a robot is the set of all such possible configurations  $q$ . To avoid collisions with any obstacles or the robot itself, typically a free space  $Q_{\text{free}} \subseteq Q$  is defined that only contains collision-free configurations.

A basic motion planning problem is defined as finding a continuous path in  $Q_{\text{free}}$  that connects from a given start configuration  $q_{\text{start}} \in Q_{\text{free}}$  to a goal configuration  $q_{\text{goal}} \in Q_{\text{free}}$ . Explicitly computing  $Q_{\text{free}}$  is a complex problem and the complexity grows with an increase of a robot's degrees of freedom [5]. We use the concept of sampling-based motion planning to avoid this by working with an implicit representation of  $Q_{\text{free}}$  probed through sampling strategies.

**Sampling-based motion planning** [23] relies on sampling collision-free configurations  $q$  in  $Q_{\text{free}}$  which are connected

to a tree or a graph. With a longer planning time and increasing numbers of samples, more space can be mapped out. If the problem is solvable, the probability of finding a path then converges to one if time goes to infinity. The algorithms provide an efficient solution for finding feasible paths for high-dimensional problems.

**Constrained planning** can be used when a robot performs tasks that limit its possible motions [19]. When we use a contact-based method with point contacts, sliding contacts or contact transitions, we put such limits on a robot's configuration space  $Q$ . In order to express these limits, we formulate a contact as a single task constraint and a transition as a set of successive task constraints. We extend the motion planning objective of finding collision-free configurations to simultaneously satisfy given constraints. These constraints are specified by a constraint function

$$f(q) : Q \rightarrow \mathbb{R}^n$$

that is satisfied when the real-value vector  $f(q) = \mathbf{0}$  for a given configuration  $q$ . This function is then used to construct an implicit constrained configuration space

$$X = \{q \in Q \mid f(q) = \mathbf{0}\}$$

. It contains all configurations that satisfy the defined constraint. We can now define a configuration space that includes all collision-free configurations from  $Q_{\text{free}}$  that also satisfy the constraints.

$$X_{\text{free}} = X \cap Q_{\text{free}}$$

A basic constrained motion planning problem is thus defined as finding a continuous path in  $X_{\text{free}}$  that connects from a given start configuration  $q_{\text{start}} \in X_{\text{free}}$  to a goal configuration  $q_{\text{goal}} \in X_{\text{free}}$ .

We assume that a robot has  $K$  **point contacts**, which are predefined points on the robots geometry. To each point contact, we associate a mapping  $f_k$  which maps a joint configuration and a surface to the distance of the  $k$ -th point contact to the nearest point on the surface. For a surface  $s$  in a workspace  $W$ , we say that the point contact fulfills a contact constraint if  $f_k(q, s) = 0$ .

A continuous motion for a contact point which fulfills the contact constraint over a surface  $s$  is a **sliding contact**. A **contact transition** is the process of breaking a contact on an initial surface  $s_I$ , moving freely and creating a contact on a goal surface  $s_G$ . In configuration space, we thereby transition from the constraint surface of all configurations  $q$  in  $Q$  for which  $f_k(q, s_I) = 0$  to being constraint-free to being in the set of configurations for which  $f_k(q, s_G) = 0$ . To keep track of sliding constraints and their transitions, we make use of the concept of a constraint graph [27], [20], which is a graph with vertices being active constraints and edges being possible transitions between active constraints.

### IV. SLIDING CONTACTS AND TRANSITION CONSTRAINTS

The goal of this work is realizing a new method for planning a single contact cycle for sliding contacts and the transition between two given contact points. For this purpose,

we develop a sliding contact constraint, a transition constraint and a sampler to efficiently exploit the transition constraint.

The sliding contact constraint keeps a contact point in constant touch with the surface of an object, while the transition constraint encompasses a contact break from a given start surface, the contact-free motion toward a goal surface and a contact creation at the goal. The steps of a transition motion is divided into three separate transition modes. We combine the concept of our contact constraint with a mode sampler that samples these three modes uniformly.

For a robot with  $K$  contact points we specify up to  $K$  fixed, sliding or transition contact constraints. Only these  $K$  designated contact points can be in contact, the rest of the body is planned to avoid any collision. In Figure 2 we show a constraint graph example for a specific robot with  $K = 2$  contact points and two contact surfaces. It depicts the three different modes a robot's contact point can be in and which modes can be accessed afterward. The  $k$ -th entry of a tuple corresponds the assignment of contact point  $k$  to the corresponding surface or to be free. In our example, each contact point can thus be in one of three modes.

- **Mode 0** contact point is unconstrained.
- **Mode 1** contact point is in contact with surface one.
- **Mode 2** contact point is in contact with surface two.

State  $(0,0)$  describes a free floating robot without any contacts. From there either contact point can make contact with object surface one or two. This mode change is depicted by the edges between the different states. State  $(1,1)$  corresponds to a robot with both contacts on the same initial surface 1 (see the green stance in Figure 3) and state  $(2,2)$  corresponds to a double contact with surface 2. A step cycle describes the process of a joint breaking contact with one surface and creating a new contact on another surface. At least one of the two joints is in contact with one of the surfaces during the whole process. A step cycle is completed by changing modes along the depicted edges starting for example at state  $(1,1)$  and ending in state  $(2,1)$ . From there, the cycle can be repeated to form a sequence of steps and transitions in context of e.g. a walking or climbing scenario.

Highlighted in green are two particular step-cycle examples we address in this work. Starting from state  $(1,1)$ , we consider the task of moving along the edges over  $(1,0)$  or  $(0,1)$  to state  $(1,2)$  or state  $(2,1)$ , respectively. This corresponds to breaking a contact point from the first surface, freely moving it and finally making contact with the second surface.

#### A. Sliding Constraint

First we present the sliding-contact constraint that is put on the  $k$ -th contact point of the robot specified to be in sliding contact. We compute the distance between this contact point and the closest point on a given surface  $S$  at the current configuration  $q$  and assign this value to the constraint function  $f_k(q, S)$ .

Algorithm 1 shows the pseudo-code for computing sliding constraints. The inputs are the robot  $r$ , the contact point on the robot  $p$  and the given contact surface  $S$ . First the contact

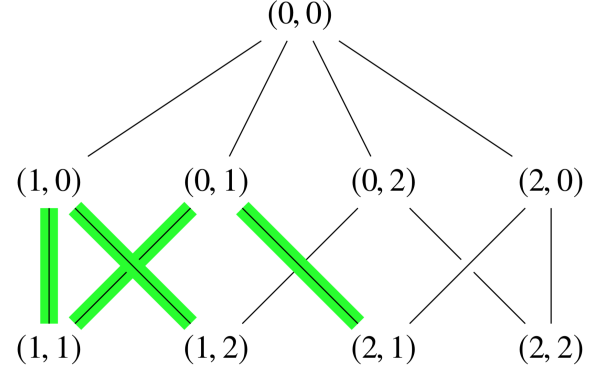


Fig. 2. Constraint Graph. This graph depicts the possible modes and mode changes of a robot with  $k = 2$  contact joints and two contact surfaces. Relevant for this work are the parts highlighted in green.

point's position in world coordinates  $p_w$  is determined. The distance  $d$  is first declared infinite. We iterate over partitions of the whole  $S$  (triangles of a given surface mesh). During each iteration we save the coordinate on one such partition  $s$  that is closest to  $p_w$  into  $c$  and the distance between these two coordinates into the variable  $d_s$ . We then compare the two distance variables and if  $d_s$  is smaller than  $d$ , we assign the value of  $d_s$  to  $d$ . After this loop, we have determined the coordinate of the surface partition closest to the current position of the robot contact joint and return this smallest distance  $d$ .

---

#### Algorithm 1: Sliding Constraint

---

**Input:** Robot  $r$ , Contact point  $p$ , Surface  $S$   
**Output:** Distance  $d$   
 $p_w \leftarrow getWorldPosition(r, p);$   
 $d = +\infty;$   
**for**  $s$  in  $S$  **do**  
     $c \leftarrow closestPosition(s, p_w);$   
     $d_s \leftarrow getDistance(c, p_w);$   
    **if**  $d_s < d$  **then**  
         $d \leftarrow d_s;$   
    **return**  $d;$

---

#### B. Transition Constraint

This section presents the implementation of our transition constraint. It combines the sliding-contact constraint with a constraint-free state into three transition modes.

Algorithm 2 shows the pseudo-code for the transition constraints. It requires input on the robot  $r$ , the contact point on the robot  $p$ , the transition mode  $mode$ , the desired contact start surface  $S_I$  and the goal surface  $S_G$ . First the contact point's position in world coordinates  $p_w$  is determined. The distance  $d$  is first declared infinite. The transition  $mode$  of the current iteration is set by our sampling method explained in the next section. We enforce a different constraint depending

on the mode. In the case of  $mode = 0$  the returned distance  $d$  is 0. This corresponds to a contact-free state and by definition the constraint is satisfied. If  $mode = 1$  then we compute a sliding-contact constraint using surface  $S_I$ . The last case of  $mode = 2$  computes a sliding constraint on surface  $S_G$ .

---

#### Algorithm 2: Transition Constraint

---

**Input:** Robot  $r$ , Contact point  $p$ , Mode  $mode$ , Start surface  $S_I$ , Goal surface  $S_G$

**Output:** distance  $d$

```

 $p_w \leftarrow getWorldPosition(r, p);$ 
if  $mode = 0$  then
| return  $d = 0$ 
else if  $mode = 1$  then
|  $d = +\infty;$ 
| for  $s$  in  $S_I$  do
| |  $c \leftarrow closestPosition(s, p_w);$ 
| |  $d_s \leftarrow getDistance(c, p_w);$ 
| | if  $d_s < d$  then
| | |  $d \leftarrow d_s;$ 
| return  $d \leftarrow d_s;$ 
else if  $mode = 2$  then
|  $d = +\infty;$ 
| for  $s$  in  $S_G$  do
| |  $c \leftarrow closestPosition(s, p_w);$ 
| |  $d_s \leftarrow getDistance(c, p_w);$ 
| | if  $d_s < d$  then
| | |  $d \leftarrow d_s;$ 
| return  $d;$ 

```

---

#### C. Sampling Method

In order to use the transition constraint for path planning, we implement a method to sample the three different constraint modes. The mode is set before calling algorithm transition and the transition constraint is enforced accordingly.

In Algorithm 3 we show the pseudo-code for sampling transition modes. The input is the configuration space  $Q$  and a list of constraints  $C$ . Each constraint could be either a fixed, sliding or a transition contact constraint. We first sample a configuration  $q$  uniform in  $Q$ . We then iterate over the constraints and check each entry if it is a transition constraint. For each transition constraint we then assign a uniformly sampled integer from  $[0, 1, 2]$  to the transition  $mode$ . Once the modes are set, we call the projection method which minimizes the constraint distance. Details on the project method can be found in [20]. To verify that we successfully projected, we then compute the distance and return the projected configuration.

#### V. EVALUATION AND RESULTS

We test our transition constraints with manipulator arms of two, three and seven internal dof and different obstacle scenarios in two-dimensional (2D) and three-dimensional (3D) space. The scenarios are run ten times with each planning algorithm and with a specified computation time. We compare

---

#### Algorithm 3: Transition Mode Sampler

---

**Input:** Configuration Space  $Q$ , Constraints  $C$

**Output:** Configuration  $q$ , Distance  $d$

```

 $q \leftarrow sampleUniform(Q);$ 
for  $c$  in  $C$  do
| if  $c$  is TransitionConstraint then
| |  $c.mode \leftarrow uniformSampledInt(0, 2);$ 
| end
|  $q \leftarrow C.project(q);$ 
|  $d \leftarrow C.distance(q);$ 
return  $q, d;$ 

```

---

the sampling-based planning algorithms Rapidly Exploring Random Tree (RRT) [21], Sparse Stable RRT (SST) [26], Search Tree with Resolution Independent Density Estimation (STRIDE) [14], Probabilistic Roadmap Method (PRM) [18] and Sparse Roadmap Spanners (SPARS) [9]. We evaluate the performance of our method by comparing the average computation times of the different algorithms.

#### A. Programming Setup

The transition contact constraints and sampler are implemented as extension of the constraint-based planning framework [20] of the Open Motion Planning Library [35], [28]. To simulate and visualize the output, we use Kris' Locomotion and Manipulation Planning Toolbox [15]. The code is written in the programming language C++ and is freely available<sup>1</sup>.

#### B. Two dof Manipulator Arm

Our first scenario is a 2D scenario with two rectangular objects and a manipulator arm with two rigid links, two joints and two contact points (yellow) to make contacts with (Figure 3). The robot starts in full contact with the lower rectangle and is required to slide along the surface with the first contact point (left), while making a sliding transition with the second contact point (right). A computed path is depicted in purple. In its goal position the robot keeps one contact with the initial surface and makes one contact with the upper rectangle.

Figure 4 shows the average computation time of ten runs of this scenario with a specified maximum planning time of two seconds. We can see that all planning algorithms find a path successfully in under a second.

#### C. Seven dof Manipulator Arm

The next scenario contains three rectangular objects and a manipulator arm with seven joints and two contact points (Figure 5). The robot starts with one contact point on the lower rectangle and the other contact point on the left-hand rectangle. The task is to transition the upper end joint toward the right-hand rectangle. To its goal position the robot has to slide the lower contact point along the lower rectangle's

<sup>1</sup>[https://github.com/mtkhoury/MotionPlanningExplorerGUI/tree/contact\\_feature](https://github.com/mtkhoury/MotionPlanningExplorerGUI/tree/contact_feature)

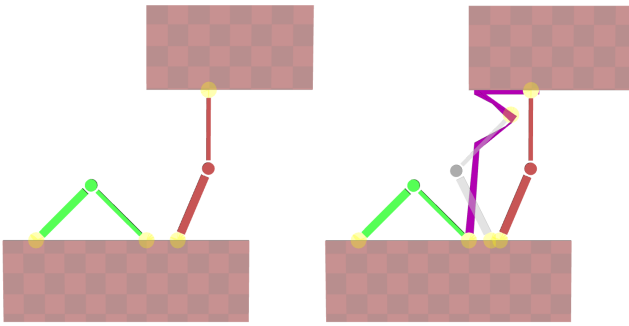


Fig. 3. Left: Two dof rectangle scenario.  $q_{start}$  is depicted in green and  $q_{goal}$  in red. Right: Path with intermediate step.

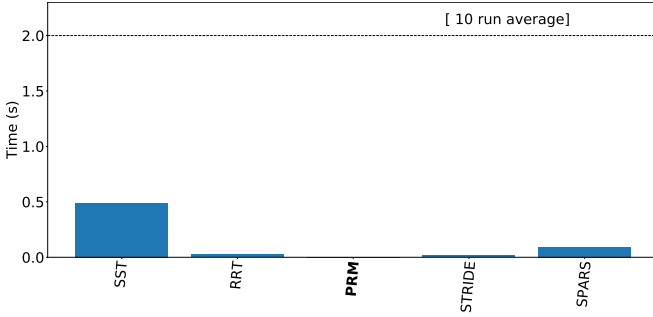


Fig. 4. Computation Time. Two dof Scenario. Maximum planning time of two seconds.

surface and has to make contact with the upper contact point on the upper right rectangle.

Figure 6 shows the ten run average computation time graph of this scenario with a specified maximum planning time of 30 seconds. We can observe that all planning algorithms find a path successfully in five seconds or less (on average). Both SPARS and SST require more time in comparison to the other three planners but they still solve the problem quickly.

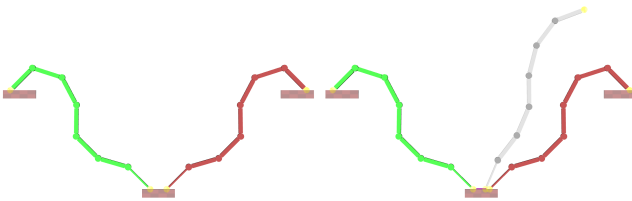


Fig. 5. Seven dof manipulator rectangle scenario.  $q_{start}$  is depicted in green and  $q_{goal}$  in red.

#### D. Three dof Manipulator Arm on Sphere

The last scenario contains a sphere, a cuboid object and a manipulator arm with three internal dof (Figure 7). The robot starts in full contact with the sphere and has to transition up along the sphere to make contact with the upper right cuboid. During the transition, we restrict one contact point to remain in sliding contact with the sphere. A path is shown on the right.

Figure 8 shows the average computation time of ten runs of this scenario with a specified maximum planning time

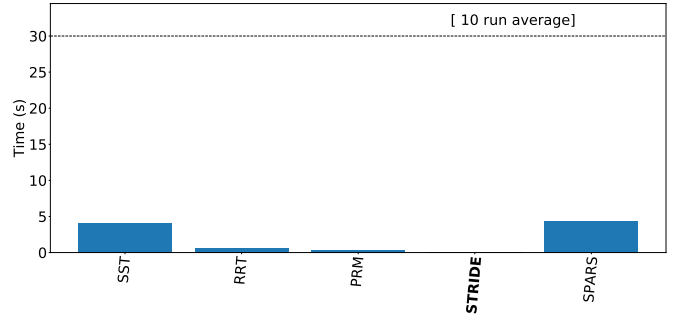


Fig. 6. Computation Time. Seven dof Scenario. Maximum planning time of 30 seconds.

of 30 seconds. We can see that not all planning algorithms find a path in the maximum planning time. The algorithms STRIDE and PRM solve the planning problem the fastest in under 5 seconds and SPARS exceeds the time limit.

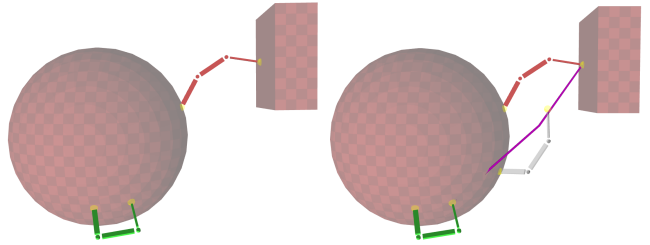


Fig. 7. Left: Three dof cuboid scenario.  $q_{start}$  is depicted in green and  $q_{goal}$  in red. Right: Path with intermediate state.

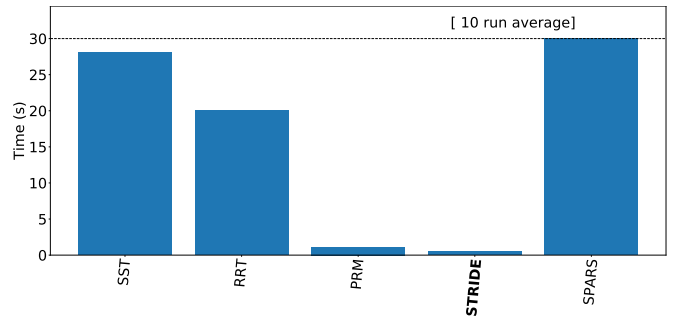


Fig. 8. Computation Time. Three dof sphere scenario. Maximum planning time of 30 seconds.

#### E. Limitations

During the setup of our testing scenarios we came across a limitation due to the different ways to set the projection. One setup, shown in Figure 9, uses the first contact point (end of thinner link) to stay in contact with the initial surface while the last contact point (end of thicker link) transitions. The other setup is vice-versa, the first contact point transitions and the last contact point keeps contact (Figure 10). Figure 11 and Figure 12 show the computation time graphs of the aforementioned setups with a maximum planning time of 30 seconds. We can see a significant difference in the planning duration until a path was found. The setup where the first

contact point is in sliding contact was solved in under two seconds by all five algorithms. In the other setup the path was found after a much longer time by three of the algorithms and the other two exceeded the maximum planning time.

This observed limitation may stem from the way the configurations are projected. In this work, we only consider setups in which the root of the robot is positioned on the robot's first contact joint. When we place the root on the robot's end joint that underlies a transition constraint, the configurations are projected differently than when this joint is constrained to be in contact with a single object's surface. We were unsure of the exact problem with the different projections and this would need to further exploration in the future.

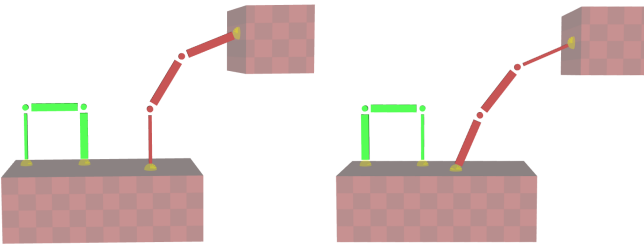


Fig. 9. Three dof with first joint in sliding contact.  $q_{\text{start}}$  is depicted in green and  $q_{\text{goal}}$  in red.

Fig. 10. Three dof with last joint in sliding contact.  $q_{\text{start}}$  is depicted in green and  $q_{\text{goal}}$  in red.

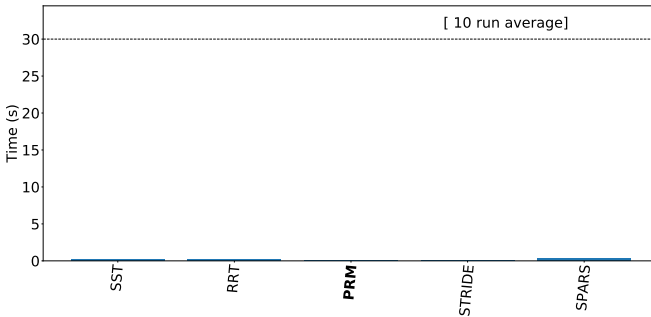


Fig. 11. Computation times for the first joint in sliding contact. Maximum planning time of 30 seconds.

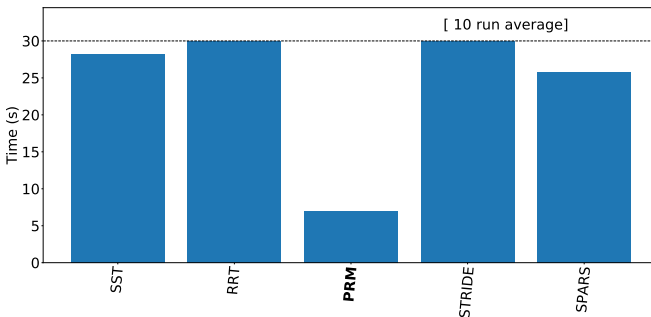


Fig. 12. Computation times for the last joint in sliding contact. Maximum planning time of 30 seconds.

Finally, we can also see that the required computation time differs depending on the scene setup. We considered

three kinds of objects in our scenarios: rectangles in the 2D scenarios, and cuboids and a sphere in the 3D scenarios. The sphere in the 3D scene leads to a longer computation time than the cuboid and rectangular objects. This could be attributed to a much higher number of surface polygons that has to be iterated over during the planning process. We also observe that planning in 2D took less time than in 3D. A 3D scenario leads to more potential contact surfaces and thus also results in more polygons. We could address this in future work using more dedicated projection methods [29].

## VI. CONCLUSION

In this work we contributed a new approach to planning sliding contacts using constrained planning and developed a sampler method for sliding transition motions. We formulated two constraints for a robot's contact joints: a sliding contact constraint and a transition constraint. For the transition constraint we split the problem into three constraint modes and implement a sampling method that samples them uniformly. We address the planning of a single contact joint breaking contact, moving it toward a goal and creating a new contact while the other joints remain in fixed or sliding contact.

Our tests and evaluations using sampling-based planning algorithms show that the presented concept works on manipulator arms in 2D and 3D scenarios. We observe that the planning time depends on the robot's body part that is set to perform the transition motion. We believe to overcome this limitation by further studying the structure of the projection itself [2], [29] or by learning explicit representations of transition constraints [12].

Despite these limitations we can successfully combine sliding contacts with contact transitions. Using this approach we are able to solve planning problems for a robot with sliding contact points, which is fundamental and could be used to plan long-horizon contact sequences.

## REFERENCES

- [1] O. M. Andrychowicz, B. Baker, M. Chociej, R. Jozefowicz, B. McGrew, J. Pachocki, A. Petron, M. Plappert, G. Powell, A. Ray *et al.*, "Learning dexterous in-hand manipulation," *International Journal of Robotics Research*, vol. 39, no. 1, pp. 3–20, 2020.
- [2] D. Berenson, S. Srinivasa, and J. Kuffner, "Task space regions: A framework for pose-constrained manipulation planning," *International Journal of Robotics Research*, vol. 30, no. 12, pp. 1435–1460, 2011.
- [3] K. Bouyarmane, S. Caron, A. Escande, and A. Kheddar, "Multi-contact motion planning and control," *Humanoid Robotics: A Reference*, pp. 1–42, 2018.
- [4] T. Bretl, "Motion planning of multi-limbed robots subject to equilibrium constraints: The free-climbing robot problem," *The International Journal of Robotics Research*, vol. 25, no. 4, pp. 317–342, 04 2006.
- [5] J. Canny, *The complexity of robot motion planning*. MIT press, 1988.
- [6] N. Chavan-Dafle, R. Holladay, and A. Rodriguez, "Planar in-hand manipulation via motion cones," *The International Journal of Robotics Research*, vol. 39, no. 2-3, pp. 163–182, 2020.
- [7] S. Cruciani, B. Sundaralingam, K. Hang, V. Kumar, T. Hermans, and D. Kragic, "Benchmarking in-hand manipulation," *Robotics and Automation Letters*, vol. 5, no. 2, pp. 588–595, 2020.
- [8] R. Deits and R. Tedrake, "Footstep planning on uneven terrain with mixed-integer convex optimization," in *IEEE International Conference on Humanoid Robots*. IEEE, 2014, pp. 279–286.
- [9] A. Dobson and K. E. Bekris, "Sparse roadmap spanners for asymptotically near-optimal motion planning," *International Journal of Robotics Research*, vol. 33, no. 1, pp. 18–47, 2014.

[10] D. Driess, P. Englert, and M. Toussaint, “Active learning with query paths for tactile object shape exploration,” in *2017 IEEE/RSJ International Conference on Intelligent Robots and Systems (IROS)*, 2017, pp. 65–72.

[11] A. Escande, A. Kheddar, and S. Miossec, “Planning contact points for humanoid robots,” *Robotics and Autonomous Systems*, vol. 61, no. 5, pp. 428 – 442, 2013.

[12] I. M. R. Fernández, G. Sutanto, P. Englert, R. K. Ramachandran, and G. S. Sukhatme, “Learning manifolds for sequential motion planning,” *arXiv preprint arXiv:2006.07746*, 2020.

[13] C. R. Garrett, R. Chitnis, R. Holladay, B. Kim, T. Silver, L. P. Kaelbling, and T. Lozano-Pérez, “Integrated task and motion planning,” *arXiv preprint arXiv:2010.01083*, 2020.

[14] B. Gipson, M. Moll, and L. E. Kavraki, “Resolution independent density estimation for motion planning in high-dimensional spaces,” in *IEEE International Conference on Robotics and Automation*. IEEE, 2013, pp. 2437–2443.

[15] K. Hauser, *Robust Contact Generation for Robot Simulation with Unstructured Meshes*. Springer International Publishing, 04 2016, vol. 114, pp. 357–373.

[16] C.-H. Hu, C.-Y. Lee, Y.-T. Liou, F.-Y. Sung, and W.-C. Lin, “Skiing simulation based on skill-guided motion planning,” in *Computer Graphics Forum*, vol. 38, no. 6. Wiley Online Library, 2019, pp. 66–78.

[17] S. Karaman and E. Frazzoli, “Sampling-based algorithms for optimal motion planning,” *International Journal of Robotics Research*, vol. 30, no. 7, pp. 846–894, 2011.

[18] L. E. Kavraki, P. Svestka, J.-C. Latombe, and M. H. Overmars, “Probabilistic roadmaps for path planning in high-dimensional configuration spaces,” *Transactions on Robotics*, vol. 12, no. 4, pp. 566–580, 1996.

[19] Z. Kingston, M. Moll, and L. E. Kavraki, “Sampling-based methods for motion planning with constraints,” *Annual Review of Control, Robotics, and Autonomous Systems*, vol. 1, no. 1, pp. 159–185, 2018.

[20] ———, “Exploring implicit spaces for constrained sampling-based planning,” *The International Journal of Robotics Research*, vol. 38, no. 10–11, pp. 1151–1178, 9 2019.

[21] J. J. Kuffner and S. M. LaValle, “RRT-connect: An efficient approach to single-query path planning,” in *IEEE International Conference on Robotics and Automation*, vol. 2, 2000, pp. 995–1001.

[22] V. Kumar, E. Todorov, and S. Levine, “Optimal control with learned local models: Application to dexterous manipulation,” in *IEEE International Conference on Robotics and Automation*. IEEE, 2016, pp. 378–383.

[23] S. M. LaValle, *Planning Algorithms*. Cambridge University Press, 2006.

[24] G. Lee, T. Lozano-Pérez, and L. P. Kaelbling, “Hierarchical planning for multi-contact non-prehensile manipulation,” in *IEEE International Conference on Intelligent Robots and Systems*. IEEE, pp. 264–271.

[25] T. Li, K. Srinivasan, M. Q.-H. Meng, W. Yuan, and J. Bohg, “Learning hierarchical control for robust in-hand manipulation,” *arXiv preprint arXiv:1910.10985*, 2019.

[26] Y. Li, Z. Littlefield, and K. E. Bekris, “Asymptotically optimal sampling-based kinodynamic planning,” *International Journal of Robotics Research*, 2016.

[27] J. Mirabel and F. Lamiraux, “Manipulation planning: addressing the crossed foliation issue,” in *IEEE International Conference on Robotics and Automation*. IEEE, 2017, pp. 4032–4037.

[28] M. Moll, I. A. Sucan, and L. E. Kavraki, “Benchmarking motion planning algorithms: An extensible infrastructure for analysis and visualization,” *IEEE Robotics Automation Magazine*, vol. 22, no. 3, pp. 96–102, 2015.

[29] A. Orthey, S. Akbar, and M. Toussaint, “Multilevel motion planning: A fiber bundle formulation,” 2020.

[30] A. Orthey and O. Stasse, “Towards reactive whole-body motion planning in cluttered environments by precomputing feasible motion spaces,” in *IEEE International Conference on Humanoid Robots*. IEEE, 2013, pp. 274–279.

[31] E. Páll, A. Sieverling, and O. Brock, “Contingent contact-based motion planning,” in *2018 IEEE/RSJ International Conference on Intelligent Robots and Systems (IROS)*. IEEE, 2018, pp. 6615–6621.

[32] O. Roussel, P. Fernbach, and M. Taix, “Motion planning for an elastic rod using contacts,” *IEEE Transactions on Automation Science and Engineering*, vol. 17, no. 2, pp. 670–683, 2019.

[33] J. Shi, J. Z. Woodruff, P. B. Umbohanowar, and K. M. Lynch, “Dynamic in-hand sliding manipulation,” *Transactions on Robotics*, vol. 33, no. 4, pp. 778–795, 2017.

[34] I. A. Sucan, M. Moll, and L. E. Kavraki, “The open motion planning library,” *IEEE Robotics Automation Magazine*, vol. 19, no. 4, pp. 72–82, 2012.

[35] S. Tonneau, A. Del Prete, J. Pettré, C. Park, D. Manocha, and N. Mansard, “An efficient acyclic contact planner for multiped robots,” *IEEE Transactions on Robotics*, vol. 34, no. 3, pp. 586–601, 2018.

[36] M. Toussaint, J.-S. Ha, and D. Driess, “Describing physics for physical reasoning: Force-based sequential manipulation planning,” *IEEE Robotics and Automation Letters*, 2020.

[37] J. C. Trinkle and R. P. Paul, “Planning for dexterous manipulation with sliding contacts,” *International Journal of Robotics Research*, vol. 9, no. 3, pp. 24–48, 1990.

[38] W. Vega-Brown and N. Roy, “Asymptotically optimal planning under piecewise-analytic constraints,” in *Algorithmic Foundations of Robotics XII*. Springer, 2020, pp. 528–543.